

# Electric-Field-Induced Fluorescence Quenching in Polyfluorene, Ladder-Type Polymers, and MEH-PPV: Evidence for Field Effects on Internal Conversion Rates in the Low Concentration Limit<sup>†</sup>

Alberto Moscatelli,<sup>‡</sup> Kathryn Livingston,<sup>‡</sup> Woong Young So,<sup>‡</sup> Suk Jun Lee,<sup>‡</sup> Ullrich Scherf,<sup>§</sup> Jurjen Wildeman,<sup>||</sup> and Linda A. Peteanu<sup>\*,‡</sup>

Department of Chemistry, Carnegie Mellon University, 4400 Fifth Avenue, Pittsburgh, Pennsylvania 15213, Bergische Universität Wuppertal, Fachbereich C - Mathematik und Naturwissenschaften Fachgebiet Makromolekulare Chemie, Gaußstraße 20, 42119 Wuppertal, Germany, and Zernike Institute for Advanced Materials, University of Groningen, Nijenborgh 4, 9747 AG Groningen, The Netherlands

Received: February 10, 2010; Revised Manuscript Received: July 27, 2010

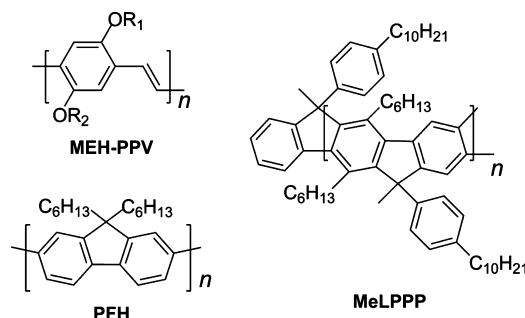
Electric field-induced fluorescence quenching has been measured for a series of conjugated polymers with applications in organic light-emitting diodes. Electrofluorescence measurements on isolated chains in a glassy matrix at 77 K show that the quenching efficiency for poly[2-methoxy-5-(2-ethylhexyloxy)-*p*-phenylenevinylene] (MEH-PPV) is an order of magnitude larger than that for either a ladder-type polymer (MeLPPP) or polyfluorene (PFH). This effect is explained in terms of the relatively high probability of field-enhanced internal conversion deactivation in MEH-PPV relative to either MeLPPP or PFH. These data, obtained under dilute sample conditions such that chain–chain interactions are minimal, are contrasted with the much higher quenching efficiencies observed in the corresponding polymer films, and several explanations for the differences are considered. In addition, the values of the change in dipole moment and change in polarizability on excitation ( $|\Delta\vec{\mu}|$  and  $tr(\Delta\vec{\alpha})$ , respectively) are reported, and trends in these values as a function of molecular structure and chain length are discussed.

## Introduction

Fluorescent conjugated polymers represent a novel class of materials<sup>1</sup> that, due to their favorable photophysical properties, have been used as the active layer in organic light-emitting diodes (OLEDs).<sup>2–5</sup> The ability to tune the intensity as well as the color of the polymer's electroluminescence is critical to developing more efficient devices. One aspect of this ongoing investigation concerns the undesirable fluorescence quenching experienced by these polymers in the external electric fields needed to drive devices.<sup>6</sup> Under these field strengths, which approach  $2 \text{ MV} \cdot \text{cm}^{-1}$ , quenching efficiencies in films of some conjugated polymers can reach 40%.<sup>7–12</sup> Though the actual magnitude of the quenching has varied among published measurements, the consensus values for poly[2-methoxy-5-(2-ethylhexyloxy)-*p*-phenylenevinylene] (MEH-PPV, Chart 1), and other PPV-type polymers lie between 10 and 20% for an applied field of  $1\text{--}2 \text{ MV} \cdot \text{cm}^{-1}$ .<sup>7,8,10,13,14</sup>

One mechanism for emission quenching in conjugated polymers is the field-induced separation of photoinduced excitons.<sup>6</sup> It is thought that electric fields of  $2 \text{ MV} \cdot \text{cm}^{-1}$  or larger can overcome the Coulombic attraction of the electron and hole pair resulting in charge separation in the excited state followed by nonradiative decay to the ground state.<sup>15</sup> Whereas the action spectra of various conjugated polymers suggest that free charges are generated on photoexcitation, whether or not this process is barrierless and the possible roles played by

CHART 1: Structure of the Polymers Used in the Present Study<sup>a</sup>



<sup>a</sup> R<sub>1</sub> = methyl, R<sub>2</sub> = 2-ethylhexyl ( $\langle n \rangle \gg 100$  for MEH-PPV,  $\langle n \rangle \sim 120$  for PFH,  $\langle n \rangle = 54$  for MeLPPP).

chain–chain interactions and defect sites within the polymer in determining its efficiency have all been sources of controversy.<sup>12,16–22</sup> Measurements of field-induced fluorescence quenching are frequently used to infer exciton binding energies ( $E_b$ ). Discrepancies between different published results have therefore contributed to the large range of values of  $E_b$  that have been quoted in the literature.<sup>17,18,20,23–25</sup> In addition to being an important parameter for device function, the magnitude of  $E_b$  determines whether a semiconductor (small  $E_b$ ) or a molecular (moderate to large  $E_b$ ) picture is most appropriate for conjugated polymers.

Previously, we showed that a second mechanism, other than field-induced exciton dissociation, contributes to the electric field-induced quenching of MEH-PPV.<sup>26</sup> Working at low temperature (77 K) in organic solvent glasses of 2-methyl tetrahydrofuran (MeTHF) with polymer concentrations at which

<sup>†</sup> Part of the "Michael R. Wasielewski Festschrift".

\* Corresponding author. Phone: 412-268-1327. Fax: 412-268-6897. E-mail: peteanu@andrew.cmu.edu.

<sup>‡</sup> Carnegie Mellon University.

<sup>§</sup> Bergische Universität Wuppertal.

<sup>||</sup> University of Groningen.

interchain interactions are negligible ( $<0.1\%$  by weight), we measured the fluorescence quenching efficiency of MEH-PPV to be  $0.6\%$  at a field of  $0.32 \text{ MV} \cdot \text{cm}^{-1}$ . If, as per refs 7, 27, and 28, the quenching scales with the square of the applied field, our measured value is equivalent to the 10–20% quenching which has been observed at the field strengths commonly used in devices ( $1\text{--}2 \text{ MV} \cdot \text{cm}^{-1}$ ).<sup>7,8,10,13,14,28</sup> More significantly, *the quenching in a 13-ring model oligomer, OPPV13, was determined to be only a factor of 2 less than that in MEH-PPV itself.* This observation is critical from the standpoint of understanding the mechanism of this process as isolated short-chain oligomers are unlikely to support exciton dissociation and charge separation on excitation to  $S_1$  in the high dielectric environment of an organic solvent glass.<sup>29</sup> We rationalized these observations by a model in which the electric field enhances the rate of internal conversion (IC) and showed that it quantitatively predicted the trend in quenching with chain length for oligomers from 5 to 13 rings as well as the polymer itself.<sup>26</sup> The IC process was presumed to occur between the optically excited  $S_1$  state and the ground state ( $S_0$ ). However, it is also possible that this process proceeds via an intermediate dark state or charge-transfer state, closer in energy to  $S_1$ , and that the applied field influences the IC process between this state and  $S_1$ .<sup>30,31</sup> Because we cannot discriminate between these two scenarios at present, the remainder of the paper refers to IC without distinguishing between the two mechanisms.

Here, this investigation is extended to other important polymers used as blue emitters in OLED devices: poly(9,9-dihexylfluorene) (PFH, Chart 1)<sup>32</sup> and methyl-substituted ladder-type poly(*p*-phenylene) (MeLPPP, Chart 1).<sup>33</sup> Unlike MEH-PPV, PFH and MeLPPP have a methylene-bridged structure that forces planarization in both the ground and excited states. Because of its low intrachain disorder and consequent vibronically well-resolved absorption and emission spectra in both solution and film, MeLPPP has been used as a model compound to elucidate photoluminescence and quenching mechanisms in conjugated fluorescent polymers.<sup>15,34–36</sup> MeLPPP<sup>12,28,37</sup> and polyfluorene-type polymers<sup>38</sup> exhibit even larger field-induced quenching efficiencies than MEH-PPV in optically dense thin films and at high field strengths, although it is generally believed that all three polymers have similar values of  $E_b$  ( $\sim 0.3\text{--}0.5 \text{ eV}$ ).<sup>39,40</sup> However, we show here that, at high dilution and lower field strengths, the field-induced quenching efficiency of these molecules is over a factor of 10 *smaller* than that observed in MEH-PPV or in any of its 5–13 ring oligomers. Generalizing from our findings in ref 26, we propose that the decreased quenching in polyfluorene and the ladder polymer relative to MEH-PPV itself is a consequence of the fact that the efficiency of IC in these molecules is *also* known to be a factor of 5–10 smaller than in MEH-PPV.<sup>41–44</sup> In other words, under our experimental conditions the applied field causes fluorescence quenching by altering the relative separation of the excited state and either a nearby dark state or the ground state. This, in turn, affects the probability of IC. Dissociation of the exciton, with concomitant loss of emission intensity, may be favored at higher field strengths, higher excitation energies, or in dense thin-film samples with a large number of chain–chain contacts.<sup>8,10,12–14,21,28,37,38,45</sup>

## Experimental Section

Electroabsorption (EA) and electrofluorescence (EF) spectra were measured using a home-built Stark spectrometer. White light from a 150 W Xe lamp (Oriel) was focused into the entrance slit of a monochromator (Acton) equipped with a grating blazed at 500 nm with  $1200 \text{ groove} \cdot \text{mm}^{-1}$  such that

the inverse linear dispersion is  $5 \text{ nm} \cdot \text{mm}^{-1}$ . Monochromatic light with spectral resolution of 5 nm was first depolarized and then horizontally polarized, using a Glan–Thompson prism, before being focused on the sample.

For EA spectra, the transmitted light was focused to a photodiode (UDT Sensors) working in photovoltaic mode. The signal, after passing through an operational amplifier, was measured using a lock-in amplifier (Stanford Instruments SR550) phased with the frequency of the oscillating electric field (465 Hz) applied to the sample and set to acquire at the second harmonic of the signal.

For EF spectra, light emitted from the sample was collected into an emission monochromator (Acton,  $600 \text{ groove} \cdot \text{mm}^{-1}$  blazed at 500 nm, spectral resolution 5 nm) and detected by a water-cooled photomultiplier tube (Hamamatsu R928) installed at the exit slit. The electric signal was preamplified (gain =  $10^6$ ) before reaching the lock-in amplifier (electric field frequency = 175 Hz). The wavelength of the incident light was chosen at the zero crossing of the EA spectrum to minimize contributions to the EF spectrum due to field effects on the absorption cross-section. This step is critical as, at other excitation wavelengths, there is an additional modulation of the EF signal in all three polymers that can be traced to the effect of the field on the absorption cross section at those excitation wavelengths. This causes the fluorescence quenching efficiency to be sharply wavelength dependent, as will be described below.

To acquire the transmission and emission spectra with no external field, a chopper (Palo Alto Research) was used in combination with the lock-in amplifier (frequency = 175 Hz). Absorption spectra were calculated from transmission spectra of the sample and the solvent alone. Samples were prepared from polymer solutions (concentration  $\sim 10^{-6} \text{ M}$ ) dissolved in MeTHF (anhydrous, inhibitor-free, Aldrich). This solvent forms a transparent glassy matrix at 77 K. Two indium tin oxide (ITO) coated quartz slides (surface resistivity =  $75\text{--}100 \Omega \cdot \text{sq}^{-1}$ , Aldrich) were sandwiched together separated by a spacer of Kapton tape (thickness = 110 or  $220 \mu\text{m}$ ). The sample was placed in between the two slides in a  $\sim 5 \times 10 \text{ mm}$  well that was cut out from the tape. The slides were held together by binder clips. The electric field was supplied by a high voltage power supply (Joseph Rolfe) and electrodes connected with the opposite ends of the bound slides. The electric field applied at the sample was up to  $0.32 \text{ MV} \cdot \text{cm}^{-1}$  and, in all cases, the signal intensity was found to scale with the square of the applied field. The sample was immersed in a liquid nitrogen Dewar equipped with transparent quartz windows on four sides (H. S. Martin). Taking into account the refractive index of liquid nitrogen, the sample cell was oriented such that the applied electric field and the electric field vector of the linearly polarized incident light were at the magic angle. For each measurement, the quadratic dependence between field strength and EA and EF signal intensities was verified (see eq 1 below), multiple scans were averaged, and the lock-in set with a time constant of 1 s and a scan length of 3 s. A home-written Labview program controlled the stepping of the monochromators and the acquisition of the trace from the lock-in amplifier.

Fluorescence lifetimes were measured using a single photon counting unit (PicoHarp 300) with time resolution of  $\sim 60 \text{ ps}$ , after reconvolution with the instrument response function. The unit was coupled with a diode laser emitting at 440 nm with a repetition rate of 20 MHz. The emission was detected through fluorescence filters using a single photon avalanche photodiode (Micro Photon Devices). Lifetime measurements at 77 K were made with the sample immersed in liquid nitrogen in an optical

dewar. Fitting of the data was performed using commercial software (Fluorofit, Picoquant). Typically either a two- or three-exponential curve was required to obtain random residuals. However, for all three polymers, only one decay time was considered meaningful. The remaining time constants either contributed very little (<2%) to the overall amplitude or were within the instrument response time. Similar values (error  $\pm 5\%$ ) were obtained by simply fitting the tail of the emission decay starting at times longer than the measured instrument response function.

MEH-PPV, MeLPPP, and the fluorene oligomers were obtained from Drs. Wildeman, Scherf, and Tagawa (Osaka University, Japan), respectively. PFH was purchased from ADS Dyes (ADS130BE; Ni content < 1 ppm) and used without further purification.

The analysis of the EA and EF data follows Liptay's treatment for isotropic samples.<sup>46–48</sup> The change in the fluorescence signal as a function of wavenumber ( $\tilde{\nu}$ ),  $\Delta I(\tilde{\nu})$ , due to the applied external electric field ( $\vec{F}$ ) is fitted by the weighted linear combination of the zeroth, first, and second derivative of the zero-field fluorescence spectrum,  $I(\tilde{\nu})$ , as described by eq 1.

$$\Delta F(\tilde{\nu}) = \vec{F}_{\text{eff}}^2 \left[ a_{\chi} F(\tilde{\nu}) + b_{\chi} \frac{\tilde{\nu}}{15\hbar c} \left\{ \frac{\partial}{\partial \tilde{\nu}} \left( \frac{F(\tilde{\nu})}{\tilde{\nu}^3} \right) \right\} + c_{\chi} \frac{\tilde{\nu}}{30\hbar^2 c^2} \left\{ \frac{\partial^2}{\partial \tilde{\nu}^2} \left( \frac{F(\tilde{\nu})}{\tilde{\nu}^3} \right) \right\} \right] \quad (1)$$

Here,  $\vec{F}_{\text{eff}} = \vec{F} \cdot \vec{f}$  and represents the effective electric field at the sample and includes the enhancement,  $f$ , due to the cavity field of the matrix. Enhancement is calculated elsewhere and is typically between 1.1 and 1.3 for most glassy matrices.<sup>49,50</sup> The subscript  $\chi$  represents the angle between the direction of the applied electric field and the electric field vector of the linearly polarized incident light. The experiments reported here were performed at the magic angle which is  $\chi = 54.7^\circ$  in air. At this angle, all terms that depend on the relative orientation of the transition moment and the applied field go to zero.

The coefficients  $a_{\chi}$ ,  $b_{\chi}$ , and  $c_{\chi}$  are functions of the transition moment polarizability ( $A_{ij}$ ) and hyperpolarizability ( $B_{ij}$ ), the average change in electronic polarizability ( $\langle \Delta \vec{\alpha} \rangle$ ), and the change in dipole moment ( $|\Delta \vec{\mu}|$ ), as given in eqs 2–4 for  $\chi = 54.7^\circ$ .

$$a_{54.7} = \frac{1}{3|\vec{m}|^2} \sum_{ij} A^2 + \frac{2}{3|\vec{m}|^2} \sum_{ij} \vec{m}_i B_{ij} \quad (2)$$

$$b_{54.7} = \frac{10}{|\vec{m}|^2} \sum_{ij} \vec{m}_i A_{ij} \Delta \vec{\mu}_j + \frac{15}{2} \langle \Delta \vec{\alpha} \rangle \quad (3)$$

$$c_{54.7} = 5|\Delta \vec{\mu}|^2 \quad (4)$$

In these equations,  $A_{ij}$  and  $B_{ij}$ , which describe the effect of  $\vec{F}_{\text{eff}}$  on the molecular transition moment ( $\vec{m}$ ), are in general quite small for allowed transitions and can therefore be neglected relative to other terms in the expression of  $b_{54.7}$ . The trace of the change in the polarizability tensor between the excited states and the ground state,  $\text{tr}(\Delta \vec{\alpha})$ , is three times the average polarizability of eq 3, i.e.  $\text{tr}(\Delta \vec{\alpha}) = 3\langle \Delta \vec{\alpha} \rangle$ . Information pertaining to  $|\Delta \vec{\mu}|$  is contained within the  $c_{54.7}$  term. In these experiments, the magnitude of  $|\Delta \vec{\mu}|$ , rather than its sign, is

measured because of the random orientation of the sample in the glassy matrix. The values for the coefficients  $a_{54.7}$ ,  $b_{54.7}$ , and  $c_{54.7}$  are extracted by using the linear least-squares fit of the EF signal using a home-written Matlab code.<sup>51</sup> In all cases, the entire EF spectrum was simulated using a single set of coefficients. This indicates that the electronic properties of the molecule are consistent across the entire fluorescence band. Analogously, the change in absorbance signal,  $\Delta A(\tilde{\nu})$ , was simulated using the same set of eqs 1–4 with the difference being that derivatives of the absorption spectrum are used in eq 1, and these are normalized to  $\tilde{\nu}$  rather than to  $\tilde{\nu}^3$ . A similar Matlab routine was used to extract  $\text{tr}(\Delta \vec{\alpha})$  and  $|\Delta \vec{\mu}|$  between the ground state and the Franck–Condon state of the  $S_1 \leftarrow S_0$  transition. Also in this case, a single set of coefficients was found to be sufficient to simulate the entire absorption band.

The magnitude of the field-induced quenching was measured by two independent methods. The first was to divide the  $a_{54.7}$  signal obtained from fitting the EF data by the peak intensity of the fluorescence spectrum and multiply by 100%. The second was to measure this quantity directly, without the need to simulate the EF spectrum, by acquiring the integrated fluorescence intensity with and without the electric field. For this measurement, the system described above was modified by replacing the emission monochromator grating with a mirror to direct all emitted light to the photomultiplier tube. The sample was oriented so that the direction of the applied field was at a magic angle to the electric field vector of the light. The signal was averaged for 20 s, and care was taken that there was no decay in the emission intensity due to photobleaching. In all cases, the two techniques gave the same results for the magnitude of the quenching within our experimental error.

## Results and Discussion

The absorption and emission spectra of each polymer obtained in MeTHF glass at 77 K (Figure 1) demonstrate that aggregation is minimal in that environment. The absorption spectrum of PFH in solvent glass (Figure 1) resembles that of the glassy or disordered phase rather than that of the  $\beta$  or highly ordered phase<sup>52,53</sup> as reported in films,<sup>45,54</sup> single chains,<sup>55</sup> and nanoaggregates.<sup>56</sup> The spectral signature of the ordered phase in absorption is a sharp transition  $\sim 2000 \text{ cm}^{-1}$  lower in energy than the more intense and broader main band that has been assigned to the glassy or disordered phase.<sup>52,53</sup> Interestingly, the emission spectrum of PFH in glass shows the overall red shift that is thought to be due to planarization of the chains in the  $\beta$ -phase.<sup>53</sup> However, it does not resemble that of solution-aggregated polyfluorene (see Supporting Information, Figure SI2) nor does it show the green emission characteristic of keto defects.<sup>57</sup> The MeLPPP sample (Figure 1 top right) also does not exhibit the red-shifted emission characteristic of aggregation (band centered at  $\sim 560 \text{ nm}$ , see Supporting Information).<sup>19</sup> The emission spectrum of MEH-PPV in glass (Figure 1 bottom left) shows a relatively intense 0–0 band compared to the vibronic replicates, suggesting a high degree of planarity though there is no evidence of the red-shifted emission characteristic of aggregates. The fluorescence spectrum of the 13-ring oligomer, OPPV13 (Figure 1), is likewise devoid of features that can be attributed to aggregation. *The absence of aggregation-induced spectral features in all three polymers suggests that their chains are well-isolated in the solvent glass environment.*<sup>12,21</sup> This point is important for understanding the mechanism of electric-field-induced quenching in these materials as described below.

The EA spectra for PFH and the ladder-type polymer are shown in Figure 2. The good match between experiment and

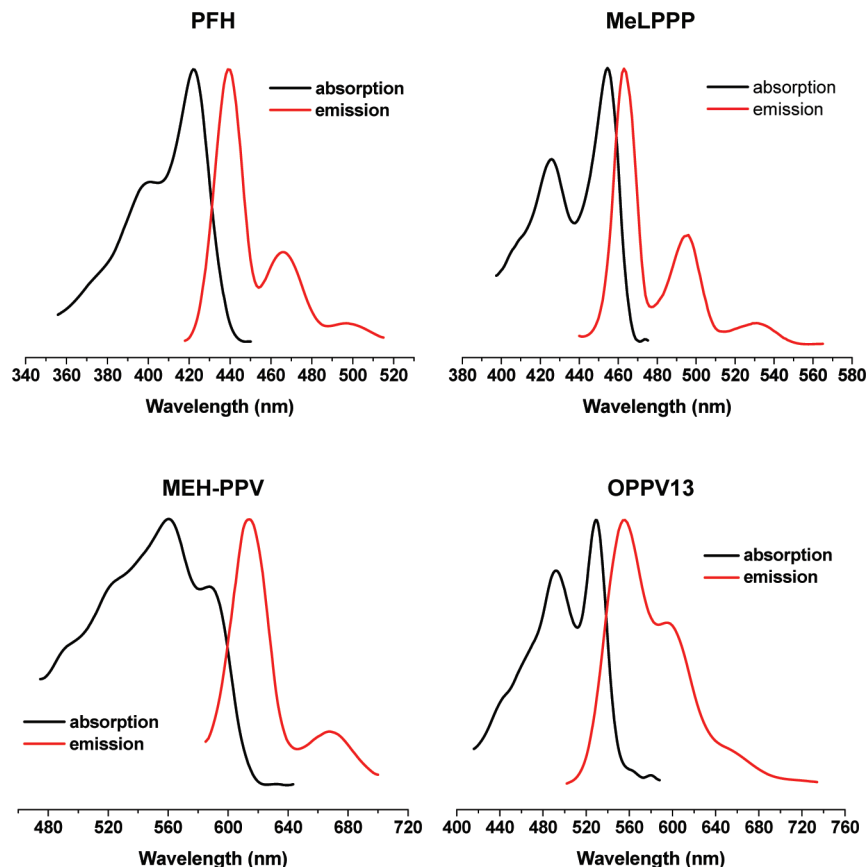


**Figure 1.** Absorption and emission spectra obtained at 77 K in MeTHF of PFH, MeLPPP, MEH-PPV, and OPPV13.

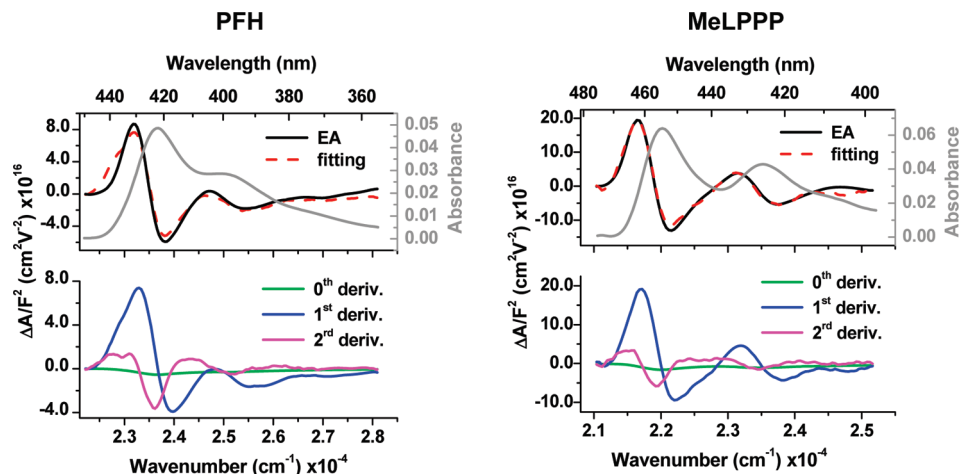


**Figure 2.** EA spectra at 77 K in MeTHF glass (black trace) and fits (dotted red trace) of PFH and MeLPPP. Also shown: absorption spectrum (gray trace) and the weighted derivative components of the absorption spectrum used in the fitting (bottom panel).

fit, especially in regard to the vibronic structure, indicates that our level of approximation is sufficient to extract meaningful values of  $|\Delta\tilde{\mu}|$  and  $tr(\Delta\tilde{\alpha})$ . Moreover, the quality of the fits suggests that the electronic properties of these materials are quite uniform over the wavelength region probed.

The EA spectrum of both polymers is dominated by the first and second derivatives of their corresponding absorption spectra, with little or no contribution from the zeroth derivative. The same pattern was observed in the EA spectrum of MEH-PPV and the related 13-ring oligomer (OPPV13).<sup>58</sup> The absence of a zeroth derivative component suggests that the transition moment of the  $S_0$  to  $S_1$  transition is unaltered in the field (see eq 2). This is an important point in the interpretation of the field-induced quenching mechanism because it implies that the

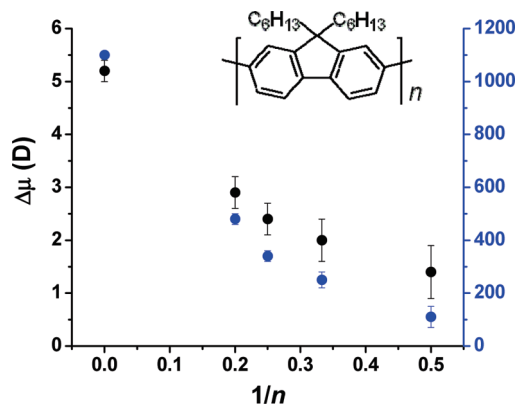
field does not alter the *radiative* rate of the transition. Moreover, it implies that the basic electronic character of the transition remains essentially unchanged, at least for the field strengths used in this experiment.

Turning to the other measured parameters (Table 1), the value of  $|\Delta\tilde{\mu}|$  is significant for all three polymers, though each is nominally  $C_{2h}$ .<sup>59</sup> For comparison, no contribution from  $|\Delta\tilde{\mu}|$  was reported in refs 45 or 54 for PFH, though an exceptionally large  $|\Delta\tilde{\mu}|$  of  $\sim 34$  D was reported for a ladder PPV in ref 35. Detailed experimental and computational studies on a model nine-ring oligomer of MEH-PPV have shown that the nonzero  $|\Delta\tilde{\mu}|$  values in these materials can be traced to the combined effects of two symmetry-breaking mechanisms: ground state structural distortions that lower the symmetry and the presence of induced dipole



**TABLE 1: Parameters Derived from Fitting the EA Spectra of Figure 2**

	$ \Delta\tilde{\mu} $ D	$tr(\Delta\tilde{\alpha})$ $\text{\AA}^3$
PFH	$5.3 \pm 0.3$	$1100 \pm 100$
MeLPPP	$3.8 \pm 0.5$	$1100 \pm 200$
MEH-PPV <sup>a</sup>	$10 \pm 1.0$	$3000 \pm 600$
OPPV13 <sup>a</sup>	$9.0 \pm 2.0$	$2000 \pm 200$

<sup>a</sup> From ref 58.**Figure 3.**  $|\Delta\tilde{\mu}|$  and  $tr(\Delta\tilde{\alpha})$  evaluated from the measured EA spectra for a series of dihexylfluorene oligomers ( $n = 2, 3, 4, 5$ ) and PFH ( $1/n$  approaching 0).

moments from the interaction of the random electrostatic dipoles of the surrounding solvent glass with this highly polarizable molecule.<sup>60</sup> Both effects were found to contribute nearly equally to the observed  $|\Delta\tilde{\mu}|$  in this oligomer. The fact that both PFH and MeLPPP have somewhat smaller values of  $|\Delta\tilde{\mu}|$  than MEH-PPV is likely due to a combination of these two factors. The  $tr(\Delta\tilde{\alpha})$  values for both polymers are roughly half that of MEH-PPV (see below), meaning that the solvent-glass-induced dipole moments will be smaller as well. Moreover, both have less conformational flexibility than MEH-PPV. Therefore, geometric distortions that would break the nominal ground state  $C_{2h}$  symmetry are less favorable. As expected from these arguments, the results of the EA simulation (Table 1) confirm a smaller  $|\Delta\tilde{\mu}|$  as one moves from a structurally more flexible MEH-PPV to the comparatively more planar PFH and MeLPPP.<sup>61</sup> We note that the value of  $|\Delta\tilde{\mu}|$  for bulk MEH-PPV is similar to that measured on single chains.<sup>62</sup>

As stated above, lower values of  $tr(\Delta\tilde{\alpha})$  are measured for PFH and MeLPPP than for MEH-PPV. The value of  $tr(\Delta\tilde{\alpha})$  reported here for PFH is consistent with that in ref 45 though smaller than that reported in ref 54 for a similar structure. For the ladder polymer, our value of  $tr(\Delta\tilde{\alpha})$  is somewhat smaller than that in ref 35. The magnitude of  $tr(\Delta\tilde{\alpha})$  is sometimes taken as a measure of electronic delocalization in the excited states of conjugated systems.<sup>63,64</sup> This has been shown previously for MEH-PPV oligomers of 5 to 13 repeat units for which  $|\Delta\tilde{\mu}|$  and  $tr(\Delta\tilde{\alpha})$  increase with chain length.<sup>26,58,60</sup> The value of  $tr(\Delta\tilde{\alpha})$  was shown to plateau at  $n \sim 13$ , where  $n$  is the number of repeat units. This chain length is in the range of the commonly accepted values for the effective conjugation length for MEH-PPV as measured by other optical techniques,<sup>65</sup> suggesting a connection between  $tr(\Delta\tilde{\alpha})$  and the excited state delocalization length.<sup>58</sup> Likewise, for PFH oligomers for up to five repeat units, EA measurements (Figure 3) show a nearly linear increase of  $|\Delta\tilde{\mu}|$  and  $tr(\Delta\tilde{\alpha})$  with chain length though the saturation length of these properties could not be examined because longer oligomers

were not available. Notably, though the value of  $tr(\Delta\tilde{\alpha})$  is well correlated with delocalization length and conductivity as long as only molecules within a given structural type are considered (i.e., OPPV chains and MEH-PPV), there appears *not* to be a strong correlation between  $tr(\Delta\tilde{\alpha})$  and charge mobility if *different* chemical species are compared. Evidence for this is the fact that the charge mobilities of MEH-PPV and PFH in isolated chains in solution, measured using time-resolved microwave conductivity (TRMC), are several orders of magnitude smaller than that of MeLPPP though all three exhibit similar values of  $tr(\Delta\tilde{\alpha})$ .<sup>66–68</sup> The EF spectra and fits (Figure 4) for MEH-PPV, PFH, and MeLPPP show once again a good match between the experimental and fitted traces indicating that eqs 1–3 are adequate to extract meaningful values of  $|\Delta\tilde{\mu}|$  and  $tr(\Delta\tilde{\alpha})$ .

The most notable difference between these three EF spectra is that *the emission of MEH-PPV is quenched significantly in the applied field, whereas that of PFH and the ladder polymer is not*. Emission quenching in MEH-PPV is apparent in that the EF spectrum, which is essentially the difference between the fluorescence spectrum in an applied field and that at zero field, closely follows the shape of the emission spectrum itself but is negative going. This is equivalent to saying that fitting the EF spectrum requires a large and negative zeroth-derivative component (green line, Figure 4). In contrast, the EF lineshapes of PFH and MeLPPP are dominated by the first-derivative component. This means that the primary effect of the applied field is to decrease the energy separation between the ground and excited states due to the difference in their respective polarizabilities. For all three polymers, the lineshapes and therefore the emission quenching efficiencies are essentially independent of the emission wavelength when the  $S_1 \leftarrow S_0$  transition is irradiated at the wavelength of the zero crossing of the EA spectrum (see Experimental Section).

The quenching efficiency,  $Q_F$ , inferred from the EF results is calculated (Table 2) using the zeroth derivative fitting weight,  $a_{54.7}$ , and eq 5.

$$Q_F = \frac{a_{54.7}}{I_0} \cdot 100 \quad (5)$$

To confirm the EF findings, the fluorescence quenching efficiency,  $Q_F$ , was measured directly (see Experimental Section) also by exciting at the wavelength of the zero crossing of the EA spectrum (Table 2). The excellent agreement between the values obtained for  $Q_F$  using these two methods confirms that the electric field quenches the emission of MEH-PPV an order of magnitude more efficiently than that of either polyfluorene or the ladder-type polymers.<sup>58</sup> Below we outline what we believe to be the mechanism of quenching under the conditions of our experiment. Next, the present results are compared to those in the literature, and hypotheses are offered for the differences observed.

Previously, we had reported that the field-induced quenching of MEH-PPV under the conditions of the current experiment (low temperature, dilute organic solvent glass matrix, and matched ITO electrodes) was only a factor of  $\sim 2$  larger than that of its 13-ring oligomer (OPPV13), for which it was presumed that exciton dissociation is unlikely, at least for isolated chains in frozen high dielectric glasses. Field-induced quenching was observed for oligomers as short as five rings and was found to increase linearly with chain length as do the values of  $|\Delta\tilde{\mu}|$  and  $tr(\Delta\tilde{\alpha})$ .<sup>58</sup> These two observations were

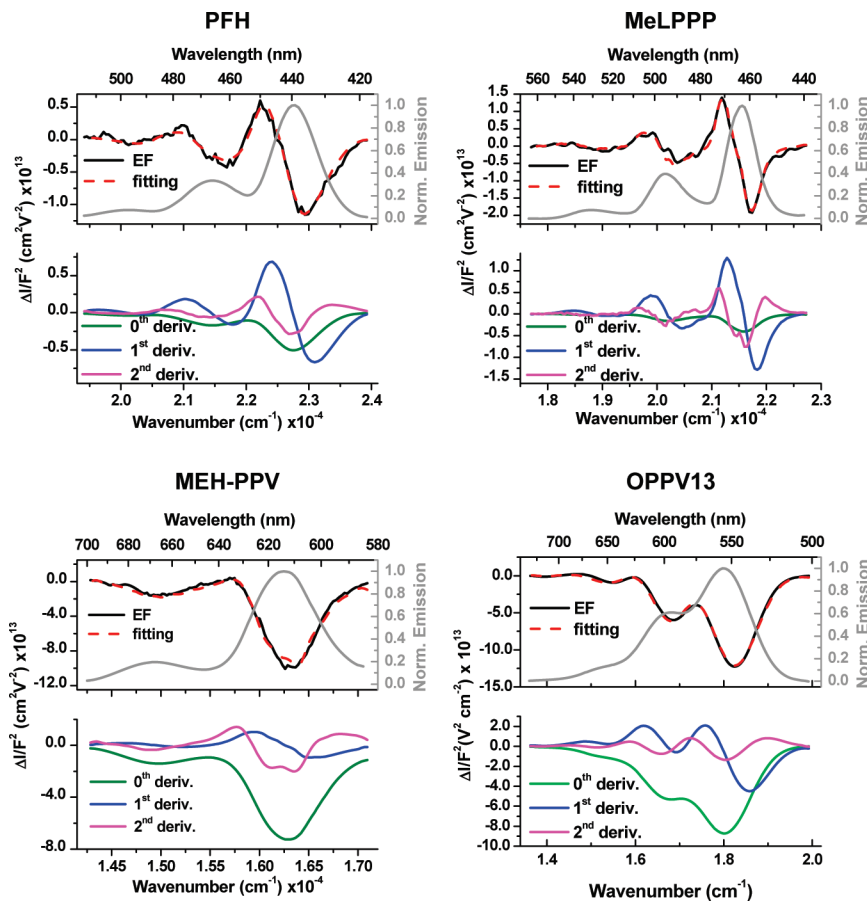


**Figure 4.** EF spectra at 77 K in MeTHF glass (black trace) and fits (dotted red trace) of PFH, MeLPPP, MEH-PPV, and OPPV13. Also shown: fluorescence spectrum (gray trace) and the weighted derivative components of the fluorescence spectrum used in the fitting (bottom panel).

**TABLE 2: Electronic Properties Derived from Fitting the EF Spectra of Figure 3 and Field-Induced Quenching Efficiencies ( $Q_F$ )**

	$ \Delta\tilde{\mu} $	$tr(\Delta\tilde{\alpha})$	$Q_F$		$\Delta\tilde{\nu}^a$
	D	$\text{\AA}^3$	% <sup>b</sup>	% <sup>c</sup>	$\text{cm}^{-1}$
PFH <sup>d</sup>	$5.4 \pm 0.8$	$1100 \pm 300$	0.04	0.05	30
MeLPPP <sup>e</sup>	$4.2 \pm 0.7$	$1300 \pm 300$	0.03	0.03	24
MEH-PPV <sup>f</sup>	$8.0 \pm 1.0$	$2200 \pm 500$	0.6	0.7	45
OPPV13 <sup>g</sup>	$9.0 \pm 2.0$	$2900 \pm 850$	0.27	0.26	50

<sup>a</sup> Stark shift calculated using eq 6. <sup>b</sup>  $Q_F$  values extracted from simulations using eq 5. <sup>c</sup>  $Q_F$  values measured experimentally by integrated emission. <sup>d</sup>  $\lambda_{\text{exc}} = 402$  nm. <sup>e</sup>  $\lambda_{\text{exc}} = 438$  or 429 nm. <sup>f</sup>  $\lambda_{\text{exc}} = 579$  or 566 nm. <sup>g</sup> From ref 26. Applied field strength is  $0.32 \text{ MV} \cdot \text{cm}^{-1}$ .

rationalized by relating the Stark shift in the excited state energy of a molecule, calculated from the interaction of the applied field with  $|\Delta\tilde{\mu}|$  and  $tr(\Delta\tilde{\alpha})$ , to the measured quenching efficiency.<sup>26</sup> This model postulates that the field-induced shift in the molecular energy levels enhances the rate of some nonradiative process, thereby quenching emission. As the literature suggests that the predominant nonradiative channel in MEH-PPV and its oligomers in a field-free environment is IC,<sup>41–44</sup> enhancement of the IC rate by the field was considered to be the most likely mechanism to explain the quenching observed in both the short-chain and polymeric species. Model calculations using literature formulations for the dependence of IC on the  $S_1$  to  $S_0$  energy gap were found to give trends consistent with those observed experimentally.<sup>26</sup>

In the present work, these studies are extended to two other polymers, MeLPPP and PFH. For both molecules, the quenching

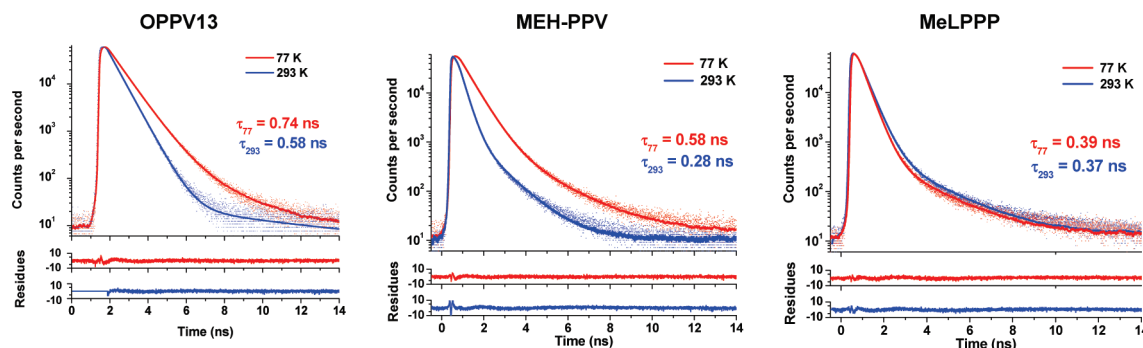
at low field strength ( $0.32 \text{ MV} \cdot \text{cm}^{-1}$ ) is below our detection limit. This is true despite the fact that their values of  $|\Delta\tilde{\mu}|$  and  $tr(\Delta\tilde{\alpha})$  are comparable to those of the 13-ring MEH-PPV oligomer (OPPV13) measured in ref 26 and for which 0.6% quenching was observed under similar conditions. Therefore, if the probability of quenching were to depend *only* on the Stark shift in the applied field, MeLPPP and PFH should exhibit at least as much quenching as OPPV13.

Table 2 contains the expected Stark shift,  $\Delta\tilde{\nu}$ , due to the measured values of  $|\Delta\tilde{\mu}|$  and  $tr(\Delta\tilde{\alpha})$  calculated from eq 6 below.

$$\Delta\tilde{\nu} = -\frac{1}{hc}|\Delta\tilde{\mu}|F - \frac{2\pi\epsilon_0}{3hc}tr(\Delta\tilde{\alpha})F^2 \quad (6)$$

where  $h$  is Planck's constant;  $c$  is the speed of light;  $\epsilon_0$  is vacuum permittivity; and  $F$  is the applied electric field strength. This represents the maximum shift that would be observed for molecules having their long axes parallel to the direction of the applied field as the change in dipole moment is roughly parallel to this axis.

For MeLPPP and PFH, the Stark shifts are somewhat smaller than those of MEH-PPV and OPPV13, and the  $S_0$  to  $S_1$  energy gaps are significantly ( $\sim 0.5$  eV) larger (see Figure 1). In a model based on the field-induced variation of the IC rate, both these factors would result in less quenching which is consistent with experiment. However, as noted above, the field-induced quenching in MeLPPP and PFH measured here is still too low compared to that of MEH-PPV and its oligomers to be accounted for simply by variations in these parameters. Rather, the results suggest that the probability of IC is *intrinsically* much smaller



**Figure 5.** Fluorescence decays following photoexcitation at 440 nm measured at 77 K (red trace) and 293 K (blue trace) in MeTHF. The fits are shown as solid lines superimposed on the data, and the residuals are shown below.

in MeLPPP and PFH than in MEH-PPV and that the applied field is therefore not strong enough to measurably affect the efficiency of the IC process.

There is, in fact, considerable evidence that the probability of IC is significantly lower in MeLPPP and PFH than in MEH-PPV or its oligomers. The photoacoustic calorimetry results of Burrows and co-workers give values for the IC yields for MEH-PPV, polyfluorene, and MeLPPP of 0.75, 0.18, and  $\sim 0$ , respectively.<sup>43</sup> This is roughly consistent with the ordering of their fluorescence yields ( $\Phi_f$ ) of 0.28, 0.79, and 0.79, respectively,<sup>43</sup> through eq 7.

$$\Phi_f = \frac{k_r}{k_r + \sum k_{nr}} = \frac{\tau_f}{\tau_r} \quad (7)$$

Here  $k_r$  is the radiative rate;  $\tau_r$  is the radiative lifetime;  $\tau_f$  is the experimentally measured fluorescence lifetime; and  $k_{nr}$  represents the rates of each of the nonradiative processes, of which IC is the fastest. Equation 7 predicts a decrease in the lifetime and in the yield with an increase in the nonradiative rate.

The possible contributions of various (temperature-dependent) nonradiative processes such as IC to the decay of the excited state can be assessed by comparing the fluorescence lifetime at room and low temperatures. Though both MEH-PPV and MeLPPP have emission lifetimes of 0.2–0.4 ns at room temperature,<sup>36,69</sup> the lifetime of the ladder polymer remains the same at 77 K, whereas that of MEH-PPV increases by nearly a factor of 2 at the lower temperature (Figure 5). A similar increase in the emission lifetime is also observed for OPPV13 (0.58 ns at 298 K and 0.74 ns at 77 K, Figure 5). This is mechanistically significant because it suggests that the temperature dependence of the lifetimes of both OPPV13 and MEH-PPV results primarily from properties *shared* between these two systems rather than from those typical only of the polymer. The latter would include a decrease in the rate of exciton migration to a quench site or to a longer segment within the polymer chain with decreasing temperature, both of which have been postulated as the mechanisms for emission quenching in MEH-PPV.<sup>44,70</sup>

We argue that the temperature dependence of the emission lifetimes of MEH-PPV and OPPV13 is due to the temperature dependence of their IC rates. The efficiency of IC typically decreases as the temperature is lowered with the magnitude of the effect depending, among other things, on the frequency of the mode(s) acting as energy acceptors.<sup>71</sup> For example, an increase of the IC rate of  $\sim 2$ – $3$  times was observed in longer-chain polyenes such as  $\beta$ -carotene in room-temperature solution versus low-temperature glass.<sup>72,73</sup> This was taken as evidence that the promoting mode for IC in this class of molecules is the

relatively low frequency C–C stretch rather than the higher frequency C–H stretch as is generally expected.<sup>71</sup> If the promoting mode for IC is actually even lower in frequency, such as a twisting about single or double bonds, the temperature dependence may be even steeper. Likewise, if there is a small barrier to IC, this can lead to temperature dependence in the rate as well.

A decrease in the IC rate in MEH-PPV and its oligomers with decreasing temperature would also cause their fluorescence lifetimes to be longer at 77 K than at room temperature (eq 7) as is observed experimentally (Figure 5). Likewise, the fact that the lifetime of MeLPPP is temperature independent over this range means that all temperature-dependent nonradiative processes are inefficient for this molecule. This together with its high emission yield at room temperature strongly implies that the  $\sim 0.4$  ns measured lifetime is the *radiative* lifetime ( $\tau_r$ ) of MeLPPP. This had been surmised earlier from theoretical calculations of the extinction coefficient, and therefore the radiative rate, as a function of chain length in ladder-type oligomers.<sup>36</sup> Unfortunately, we were unable to perform similar experiments on PFH because the wavelength of our source is too long to excite this molecule efficiently.

It may be possible to explain the large difference between the probability of IC in the more flexible structures (MEH-PPV, OPPV13) and the more rigid structures (MeLPPP, PFH), if the IC process is enhanced by the greater structural flexibility of the PPVs. For example, calculations have shown that polyenes in their  $S_1$  states experience structural distortions such as torsions and/or pyramidalization of carbons in the chain (termed “kinks”) which brings them to a conical intersection that connects directly to the ground state.<sup>74</sup> This, in turn, provides an efficient pathway for IC. Ample space for a motion of this type is available in the frozen glass as there is precedent in the literature for even larger structural changes, such as *cis*–*trans* isomerizations, occurring in confined media.<sup>75,76</sup> Interestingly, the importance of charge-transfer states in determining the characteristics of the conical intersection in polyenes has also been described.<sup>30,31</sup> If this were to apply to PPV-like structures, it would provide a rationale for the field effects on the emission yields observed here.

In summary, the picture that emerges from these and earlier studies is that, under the field strengths and sample conditions used in our experiments, *the magnitude of the field-induced quenching observed for a given conjugated polymer or oligomer on excitation to the  $S_1$  state can be understood by considering the intrinsic probability of IC in that molecule, the  $S_1$ – $S_0$  energy gap, and the Stark shift of the emitting state in the applied field.* Therefore, a significant proportion of the field-induced quenching observed in these materials can be explained by processes



that are intrinsic to the single isolated (oligomeric) chain. There is of course the potential for even greater quenching to be observed at higher field strengths, higher excitation energies, or in dense thin-film samples with a large number of chain–chain contacts.<sup>7,8,10,12–14,21,27,28,37,38,45</sup>

Below we will briefly compare our results for the magnitude of the field-induced quenching in MeLPPP and PFH to others in the literature. This comparison was discussed extensively for MEH-PPV in ref 58 and will not be repeated here, except to state that our results for MEH-PPV (Table 2) lie within the range of those presented for PPV-type polymers when the difference in field strength is accounted for by scaling by the square of the applied field ( $F$ ).<sup>7,8,10,13</sup>

Unlike what was seen for MEH-PPV, our values for the field-induced quenching efficiencies in PFH and MeLPPP (Table 2) are at least an order of magnitude smaller than those reported in the literature. For example, in dense films of MeLPPP, emission quenching efficiencies of 40% for applied fields of  $2 \text{ MV} \cdot \text{cm}^{-1}$  have been reported,<sup>12,37</sup> which is very similar to the values reported for MEH-PPV under similar conditions.<sup>7,8,10,13,14,27</sup> In polyfluorene-type polymers, Rothe et al. measured  $\sim 40\%$  quenching at  $1 \text{ MV} \cdot \text{cm}^{-1}$ .<sup>38</sup> Mehata et al. obtained a similar value in polyfluorene but measured essentially *no* quenching at lower field strengths.<sup>45</sup> Using the expected  $F^2$  field dependence,<sup>27</sup> these quenching efficiencies would scale to  $\sim 4\%$  at  $0.32 \text{ MV} \cdot \text{cm}^{-1}$ , the highest field strength used in the current experiment. This is still 2 orders of magnitude larger than what we observe. Even when the field strength dependence is assumed to be  $F^4$ , as has been suggested in ref 45, the predicted quenching ( $\sim 0.3\%$ ) is still an order of magnitude larger than that measured here. Therefore, simply scaling the field strength down to the values used in the current experiments does *not* explain the differences between the field-induced quenching measured here for PFH and MeLPPP and those in the literature. This suggests that the mechanism for quenching, at least in these two polymers, is fundamentally different at the low and high field strengths and/or that other differences in the experimental methodology are important. Below we enumerate several factors that may explain the differences between the results reported here and those in the literature.

(1) It is possible that there is a threshold field strength for field-induced exciton dissociation below which the field simply acts to perturb the energy levels via the Stark shift. At present, this is difficult to test for samples in organic glasses as higher field strengths lead to dielectric breakdown, though a thorough examination of the process at low field strengths in bulk films may yield some insight.

(2) Sample concentration may affect the field-induced quenching by enhancing the probability of interactions between polymer chains. The literature results discussed above were obtained on polymers in bulk films which, due to their high density, permit numerous chain–chain contacts and, in some cases, contain aggregated chains.<sup>7,8,10,12–14,27,37,38,45</sup> In contrast, at the low concentrations used in the current study, the average separation between polymer chains should be over an order of magnitude greater than in bulk films,<sup>58</sup> particularly as there is no spectroscopic evidence of aggregation in our samples (Supporting Information). The importance of chain–chain interactions in producing efficient quenching is illustrated in the work of Deussen et al.<sup>27</sup> who reported a pronounced concentration dependence of the field-induced quenching in a PPV-type polymer. These authors argued that chain–chain interactions enhance the probability of field-induced quenching by allowing the separation of charge onto adjacent chains. The contribution

to the quenching due to *inter-chain* induced charge separation is minimized in the dilute solvent glass environment used here which could explain the lower quenching efficiencies we observe. In addition, there may be effects due to the properties of the solvent used to prepare the samples as the conformation and folding of conjugated materials are known to be sensitive to the solvent environment. The effect of polymer conformation on field-induced quenching is, in fact, a potentially interesting area to be explored. Interestingly, field-induced quenching has also been observed in *single* polymers of MEH-PPV and MeLPPP using single-molecule microscopy.<sup>11,77,78</sup> Its magnitude is typically linear in the applied field and depends on the field polarity. Such effects are not observed in our experiments due to the random orientation of the molecules within the glass (see eq 1). Moreover, single molecule fluorescence quenching has sometimes been attributed to charge injection from the electrodes leading to the formation of a polaronic quench site.<sup>77</sup> This is a fundamentally different mechanism than has been discussed for bulk films. It would not apply in the experiments reported here because of the low probability for either charge buildup or injection in the sample when matched planar ITO electrodes and an electric field that oscillates in polarity are used.

(3) The way in which the field is applied to the sample may affect the field-induced quenching. In all of the literature reports of field-induced quenching that we are aware of, the electrodes were deposited onto the polymer films, either directly or with thin blocking layers applied. In the measurements presented here, the majority of the polymer chains lies within the dielectric glass rather than at the electrode surface. As the effects of polymer–electrode surface interactions are of considerable interest, whether or not these interactions also play a role in determining the electric-field-induced quenching behavior of polymer films is a topic worthy of investigation.<sup>34,79,80</sup>

(4) The choice of the excitation wavelength greatly affects the electrofluorescence spectrum and the magnitude of the field-induced quenching. Experimentally, *the quenching efficiency can vary by over an order of magnitude depending on the excitation wavelength used* independent of whether the quenching is measured by fitting the EF spectrum or by measuring the loss in total emission in the applied field. As one example, the total quenching measured for MeLPPP at an excitation wavelength away from the zero crossing of the EA spectrum ( $\lambda_{\text{exc}} = 456 \text{ nm}$ , Figure 2) is an order of magnitude *larger* than that measured at the zero-crossing ( $\lambda_{\text{exc}} = 429 \text{ nm}$ , Figure 2). Note that this trend is the reverse of what is expected if the amount of excess energy alone were to determine the quenching efficiency. These results illustrate that care must be taken to properly select the excitation wavelength in measurements of this type to avoid any contribution from the Stark shift of the absorption spectrum. Nevertheless, measurements of the wavelength dependence of the quenching efficiency can be very useful in establishing its mechanism once this effect is properly accounted for. These are underway in our laboratory.

## Conclusions

The EF spectra of three widely used materials in organic LED devices, namely, MEH-PPV, polyfluorene, and ladder-type polymers, reflect the structural differences among them. Whereas isolated chains of MEH-PPV show a marked fluorescence quenching upon applying a relatively weak electric field, both PFH and MeLPPP do not. The fluorescence quenching of MEH-PPV, already thoroughly investigated in a previous publication,<sup>26</sup> was explained in terms of an enhanced IC rate due to excited state stabilization in the presence of an electric field. Here, the



paradigm is extended to two other polymers that are forced into a more planar structure due to the methylene bridges between the conjugated rings. Both PFH and MeLPPP have much lower IC efficiencies than MEH-PPV, and consistent with the predictions of our previously described model,<sup>26</sup> their electric-field-induced quenching efficiencies are *also* an order of magnitude smaller than for MEH-PPV.

**Acknowledgment.** We acknowledge NSF CHE-079112 for financial support. Acknowledgment is also made to the Donors of the American Chemical Society Petroleum Research Fund for support of this research (PRF# 44317-AC4). In addition, we would like to thank Dr. David Yaron (CMU) for helpful comments and Dr. Ferdinand Grozema (Delft University of Technology) for his help in obtaining the samples used here.

**Supporting Information Available:** Emission spectra of MeLPPP and PFH in their aggregated form. This material is available free of charge via the Internet at <http://pubs.acs.org>.

## References and Notes

- Burroughes, J. H.; Bradley, D. D. C.; Brown, A. R.; Marks, R. N.; Mackay, K.; Friend, R. H.; Burns, P. L.; Holmes, A. B. *Nature* **1990**, *347*, 539.
- Braun, D.; Heeger, A. J. *App. Phys. Lett.* **1991**, *58*, 1982.
- Mitschke, U.; Bäuerle, P. *J. Mater. Chem.* **2000**, *10*, 1471.
- Grimsdale, A.; Müllen, K. *Adv. Polym. Sci.* **2006**, *199*, 1.
- Organic light-emitting devices: synthesis, properties, and applications*; Müllen, K.; Scherf, U., Eds.; Wiley-VCH: Weinheim, 2006.
- Kersting, R.; Lemmer, U.; Deussen, M.; Bakker, H. J.; Mahrt, R. F.; Kurz, H.; Arkhipov, V. I.; Bäessler, H.; Göbel, E. O. *Phys. Rev. Lett.* **1994**, *73*, 1440.
- Deussen, M.; Scheidler, M.; Bäessler, H. *Synth. Met.* **1995**, *73*, 123.
- Esteghamatian, M.; Popovic, Z. D.; Xu, G. *J. Phys. Chem.* **1996**, *100*, 13716.
- Khan, M. I.; Renak, M. L.; Bazan, G. C.; Popovic, Z. *J. Am. Chem. Soc.* **1997**, *119*, 5344.
- Khan, M. I.; Bazan, G. C.; Popovic, Z. D. *Chem. Phys. Lett.* **1998**, *298*, 309.
- McNeill, J. D.; O'Connor, D. B.; Adams, D. M.; Barbara, P. F.; Kummer, S. B. *J. Phys. Chem. B* **2001**, *105*, 76.
- Haugeneder, A.; Lemmer, U.; Scherf, U. *Chem. Phys. Lett.* **2002**, *351*, 354.
- Arkhipov, V. I.; Bäessler, H.; Deussen, M.; Goebel, E. O. *Phys. Rev. B* **1995**, *52*, 4932.
- Pfeffer, N.; Neher, D.; Remmers, M.; Poga, C.; Hopmeier, M.; Mahrt, R. *Chem. Phys.* **1998**, *227*, 167.
- Stampfl, J.; Graupner, W.; Leising, G.; Scherf, U. *J. Lumin.* **1995**, *63*, 117.
- Antoniadis, H.; Rothberg, L. J.; Papadimitrakopoulos, F.; Yan, M.; Galvin, M. E.; Abkowitz, M. A. *Phys. Rev. B* **1994**, *50*.
- Arkhipov, V. I.; Bäessler, H. *Status Solidi A* **2004**, *201*, 1152.
- Chandross, M.; Mazumdar, S.; Jeglinski, S.; Wei, X.; Vardeny, Z. V.; Kwock, E. W.; Miller, T. M. *Phys. Rev. B* **1994**, *50*, 14702.
- Kohler, A.; Gruner, J.; Friend, R. H.; Mullen, K.; Scherf, U. *Chem. Phys. Lett.* **1995**, *243*, 456.
- Bredas, J. L.; Cornil, J.; Heeger, A. J. *Adv. Mater.* **1996**, *8*, 447.
- Kohler, A.; Dos Santos, D. A.; Beljonne, D.; Shuai, Z.; Bredas, J. L.; Holmes, A. B.; Kraus, A.; Mullen, K.; Friend, R. H. *Nature* **1998**, *392*, 903.
- Moses, D.; Wang, J.; Heeger, A. J.; Kirova, N.; Brazovski, S. *Synth. Met.* **2001**, *125*, 93.
- Leng, J. M.; Jeglinski, S.; Wei, X.; Benner, R. E.; Vardeny, Z. V.; Guo, F.; Mazumdar, S. *Phys. Rev. Lett.* **1994**, *72*, 156.
- Campbell, I. H.; Hagler, T. W.; Smith, D. L.; Ferraris, J. P. *Phys. Rev. Lett.* **1996**, *76*, 1900.
- Moses, D.; Wang, J.; Heeger, A. J.; Kirova, N.; Brazovski, S. *Synth. Met.* **2001**, *119*, 503.
- Smith, T. M.; Kim, J.; Peteanu, L. A.; Wildeman, J. J. *Phys. Chem. C* **2007**, *111*, 10119.
- Deussen, M.; Haring Bolivar, P.; Wegmann, G.; Kurz, H.; Bäessler, H. *Chem. Phys.* **1996**, *207*, 147.
- Schweitzer, B.; Arkhipov, V. I.; Bäessler, H. *Chem. Phys. Lett.* **1999**, *304*, 365.
- Lüer, L.; Egelhaaf, H.-J.; Oelkrug, D.; Gadermaier, C.; Cerullo, G.; Lanzani, G. *Phys. Rev. B* **2003**, *68*, 155313/1.
- Sanchez-Galvez, A.; Hunt, P.; Robb, M. A.; Olivucci, M.; Vreven, T.; Schlegel, H. B. *J. Am. Chem. Soc.* **2000**, *122*, 2911.
- Levine, B. G.; Martinez, T. J. *Annu. Rev. Phys. Chem.* **2007**, *58*, 613.
- Polyfluorenes*; Scherf, U.; Neher, D., Eds.; Adv. Poly. Sci. Series; Springer: Berlin, 2008; Vol. 212.
- Scherf, U.; Müllen, K. *Adv. Polym. Sci.* **1995**, *123*, 1.
- Barth, S.; Bäessler, H.; Scherf, U.; Müllen, K. *Chem. Phys. Lett.* **1998**, *288*, 147.
- Harrison, M. G.; Möller, S.; Weiser, G.; Urbasch, G.; Mahrt, R. F.; Bäessler, H.; Scherf, U. *Phys. Rev. B* **1999**, *60*, 8650.
- Rissler, J.; Bassler, H.; Gebhard, F.; Schwerdtfeger, P. *Phys. Rev. B* **2001**, *64*, 045122-1.
- Tasch, S.; Kranzelbinder, G.; Leising, G.; Scherf, U. *Phys. Rev. B* **1997**, *55*, 5079.
- Rothe, C.; King, S. M.; Monkman, A. P. *Phys. Rev. B* **2005**, *72*, 085220/1.
- Alvarado, S. F.; Seidler, P. F.; Lidzey, D. G.; Bradley, D. D. C. *Phys. Rev. Lett.* **1998**, *81*, 1082.
- van der Horst, J.-W.; Bobbert, P. A.; Michels, M. A. J.; Bassler, H. *J. Chem. Phys.* **2001**, *114*, 6950.
- Oelkrug, D.; Tompert, A.; Gierschner, J.; Egelhaaf, H. J.; Hanack, M.; Hohloch, M.; Steinhuber, E. *Proc. SPIE Int. Soc. Opt. Eng.* **1997**, *3145*, 242.
- Peeters, E.; Ramos, A. M.; Meskers, S. C. J.; Janssen, R. A. J. *J. Chem. Phys.* **2000**, *112*, 9445.
- Burrows, H. D.; Seixas de Melo, J.; Serpa, C.; Arnaut, L. G.; Monkman, A. P.; Hamblett, I.; Navarathnam, S. *J. Chem. Phys.* **2001**, *115*, 9601.
- Hsu, J.-H.; Hayashi, M.; Lin, S.-H.; Fann, W.; Rothberg, L. J.; Perng, G.-Y.; Chen, S.-A. *J. Phys. Chem. B* **2002**, *106*, 8582.
- Mehata, M. S.; Hsu, C. S.; Lee, Y. P.; Ohta, N. *J. Phys. Chem. C* **2009**, *113*, 11907.
- Liptay, W. *Modern Quantum Chemistry: Istanbul Lectures: Action of Light and Organic Crystals*; Sinanoglu, O., Ed.; Academic Press: New York, 1965; Vol. 3, pp 93–138.
- Liptay, W. *Angew. Chem., Int. Ed.* **1969**, *8*, 177.
- Liptay, W. *Excited States*; Lim, E. C.; Innes, K. K., Eds.; Academic Press: New York; London, 1974; Vol. 1, pp 129–229.
- Bublitz, G. U.; Boxer, S. G. *Annu. Rev. Phys. Chem.* **1997**, *48*, 213.
- Boxer, S. G. *J. Phys. Chem. B* **2009**, *113*, 2972.
- Smith, T. M. C. *Spectral Properties and Photophysics of Conjugated Polymers in Electric Fields*; Carnegie Mellon University: Pittsburgh, PA, 2006.
- Grell, M.; Bradley, D. D. C.; Ungar, G.; Hill, J.; Whitehead, K. S. *Macromolecules* **1999**, *32*, 5810.
- Scherf, U.; List, E. J. W. *Adv. Mater.* **2002**, *14*, 477.
- Cadby, A. J.; Lane, P. A.; Mellor, H.; Martin, S. J.; Grell, M.; Giebeler, C.; Bradley, D. D. C.; Wohlgenannt, M.; An, C.; Vardeny, Z. V. *Phys. Rev. B* **2000**, *62*, 15604.
- Becker, K.; Lupton, J. M. *J. Am. Chem. Soc.* **2005**, *127*, 7306.
- Wu, C.; McNeill, J. *Langmuir* **2008**, *24*, 5855.
- Becker, K.; Lupton, J. M.; Feldmann, J.; Nehls, B. S.; Galbrecht, F.; Guo, D.; Scherf, U. *Adv. Funct. Mater.* **2006**, *16*, 364.
- Smith, T. M.; Hazelton, N.; Peteanu, L. A.; Wildeman, J. J. *Phys. Chem. B* **2006**, *110*, 7732.
- Atkins, P.; Friedman, R. *Molecular Quantum Mechanics*; Oxford Univ. Press: Oxford, 2007.
- Wachsmann-Hogiu, S.; Peteanu, L. A.; Liu, L. A.; Yaron, D. J.; Wildeman, J. J. *Phys. Chem. B* **2003**, *107*, 5133.
- Schindler, F.; Lupton, J. M.; Feldmann, J.; Scherf, U. *Proc. Natl. Acad. Sci.* **2004**, *101*, 14695.
- Schindler, F.; Lupton, J. M.; Muller, J.; Feldmann, J.; Scherf, U. *Nat. Mater.* **2006**, *5*, 141.
- Horvath, A.; Bassler, H.; Weiser, G. *Phys. Status Solidi B* **1992**, *173*, 755.
- Gelinck, G. H.; Piet, J. J.; Wegewijs, B. R.; Mullen, K.; Wildeman, J.; Hadzioannou, G.; Warman, J. M. *Phys. Rev. B* **2000**, *62*, 1489.
- Woo, H. S.; Lhost, O.; Graham, S. C.; Bradley, D. D. C.; Friend, R. H.; Quattrocchi, C.; Bredas, J. L.; Schenk, R.; Müllen, K. *Synth. Met.* **1993**, *59*, 13.
- Grozema, F. C.; Warman, J. M. *Radiat. Phys. Chem.* **2005**, *74*, 234.
- Prins, P.; Grozema, F. C.; Schins, J. M.; Patil, S.; Scherf, U.; Siebbeles, L. D. A. *Phys. Rev. Lett.* **2006**, *96*, 146601/1.
- Prins, P.; Grozema, F. C.; Siebbeles, L. D. A. *J. Phys. Chem. B* **2006**, *110*, 14659.
- Smilowitz, L.; Hays, A.; Heeger, A. J.; Wang, G.; Bowers, J. E. *J. Chem. Phys.* **1993**, *98*, 6504.
- Rassamesard, A.; Huang, Y.-F.; Lee, H.-Y.; Lim, T.-S.; Li, M. C.; White, J. D.; Hodak, J. H.; Osotchan, T.; Peng, K. Y.; Chen, S. A.; Hsu, J.-H.; Hayashi, M.; Fann, W. *J. Phys. Chem. C* **2009**, *113*, 18681.

- (71) Engleman, R.; Jortner, J. *Mol. Phys.* **1970**, *18*, 145.
- (72) Wasielewski, M. R.; Johnson, D. G.; Bradford, E. G.; Kispert, L. D. *J. Chem. Phys.* **1989**, *91*, 6691.
- (73) Andersson, P. O.; Bachilo, S. M.; Chen, R.-L.; Gillbro, T. *J. Phys. Chem.* **1995**, *99*, 16199.
- (74) Bernardi, F.; Olivucci, M.; Robb, M. A. *Chem. Soc. Rev.* **1996**, *25*, 321.
- (75) Kohler, B. E. *Chem. Rev.* **1993**, *93*, 41.
- (76) Liu, R. S. H.; Yang, L.-Y.; Liu, J. *Photochem. Photobiol.* **2007**, *83*, 2.
- (77) Scheblykin, I.; Zorinants, G.; Hofkens, J.; De Feyter, S.; Van der Auweraer, M.; De Schryver, F. C. *ChemPhysChem* **2003**, *4*, 260.
- (78) Schindler, F.; Lupton, J. M.; Feldmann, J. *Chem. Phys. Lett.* **2006**, *428*, 405.
- (79) Becker, H.; Lux, A.; Holmes, A. B.; Friend, R. H. *Synth. Met.* **1997**, *85*, 1289.
- (80) Sheats, J. R.; Chang, Y.-L.; Roitman, D. B.; Stocking, A. *Acc. Chem. Res.* **1999**, *32*, 193.

JP101307P